Available online at www.sciencedirect.com
SCIENCE DIRECT
Journal of Catalysis 238 (2006) 6–12
JOURNAL OF CATALYSIS
www.elsevier.com/locate/jcat

Dehydration of phenyl-ethanol to styrene: Zeolite catalysis under reactive distillation

Jean-Paul Lange *, Vincent Otten [1]

Shell Global Solutions, Badhuisweg 3, 1031 CM Amsterdam, The Netherlands

Received 27 June 2005; revised 21 November 2005; accepted 23 November 2005

Available online 22 December 2005

Abstract

Styrene is commercially produced by the dehydration of phenyl-ethanol with co-production of propene oxide. We investigated the possibility of carrying out this reaction at mild temperatures under reactive distillation conditions. Medium-pore zeolites, such as H-ZSM-5 and H-ZSM-11, were found to be very active and selective at 170 °C. The Lewis-acidic TS-1 zeolite showed similarly high selectivity but lower activity. High activity and selectivity required small (<50 nm) zeolite crystals. In contrast, large-pore zeolites and mesoporous solid acids did not produce much styrene under these conditions. These results show the importance of shape selectivity. The styrene selectivity rapidly degraded with time on stream, however, leading to the formation of ethers and, subsequently, styrene oligomers. No simple model can explain all of the factors affecting ether formation.

Keywords: Styrene; Phenyl-ethanol; Reactive distillation; Zeolite; ZSM-5; TS-1; Ether; Shape-selectivity; Deactivation; Crystal size; Diffusion

1. Introduction

The major commercial route toward styrene is based on the catalytic dehydrogenation of ethylbenzene, which was discovered and developed by IG Farben in the 1930s [1,2]. Less important manufacturing routes via the dehydration of 1-phenyl-ethanol, Φ–CH(OH)–CH_3, have been ongoing for some time. In the 1940s, Union Carbide Chemicals commercialised a styrene process based on the oxidation of ethylbenzene to acetophenone, Φ–C(O)–CH_3, followed by selective hydrogenation to 1-phenyl-ethanol and finally dehydration to styrene [2,3]. The dehydration step proceeded in the vapour phase by passing the alcohol over a titania catalyst at 200–250 °C. Poor overall yields and corrosion problems made this oxidation route obsolete.

In the mid 1970s, however, a route based on the co-production of styrene and propylene oxide was discovered by Halcon and improved by Shell [1]. It involved the oxidation of ethylbenzene with air to its hydroperoxide, a subsequent oxygen transfer between the hydroperoxide and propene to form 1-phenyl-ethanol and propene oxide and, finally, the dehydration of 1-phenyl-ethanol to styrene (Fig. 1). Although less extensively applied than the direct dehydrogenation route, the co-production route is steadily gaining in importance.

The styrene/propene oxide co-production route uses a titania- or alumina-based catalyst for dehydrating 1-phenyl-ethanol in the gas phase at ∼300 °C [1,4,5]. The peculiarity of these catalysts relies not on their activity, but rather on their styrene selectivity and their low tendency to produce oligomeric materials that would otherwise deactivate the catalyst. More acidic materials, such as amorphous silica–aluminas and zeolites, are reportedly more active than alumina and titania but show clear signs of deactivation after just 1 h of operation [6,7]. Recently, we succeeded in extending the lifetime of ZSM-5-based catalysts beyond 150 h, with high conversion (>90%) and high selectivity (>90%), by improving the diffusion characteristics of the catalyst particle [8,9]. The slow diffusion of styrene through the mesopores of the bound-zeolite catalyst was indeed found to be responsible for the formation of styrene oligomers and the resulting poisoning of the catalyst.

* Corresponding author. Fax: +31 20 630 8004.
E-mail address: jean-paul.lange@shell.com (J.-P. Lange).
[1] Present address: AC Analytical Controls, Innsbruckerweg 35, 3047 AG, Rotterdam, The Netherlands.

0021-9517/$ – see front matter
doi:10.1016/j.jcat.2005.11.033

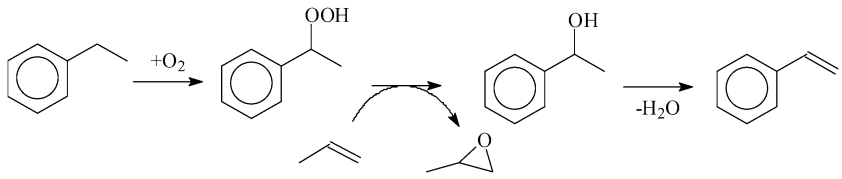

Fig. 1. The SM/PO process for the co-production of styrene and propene oxide.

Pursuing this lead, we explored the possibility of further improving the selectivity of the reaction by removing styrene from the reaction mixture through reactive distillation. Distillative separation of styrene and 1-phenyl-ethanol is facile given their respective atmospheric boiling points of 145 and 203 °C. In this study, we revisited a number of zeolites and other strong solid acids and specifically investigated the influence of Si/Al ratio, pore size, and crystal size on catalytic performance.

2. Experimental

The reactions were carried out in a three-necked, round-bottomed flask (250 mL), which was heated by an oil-bath and equipped with a small rectification column (100 mm long and 15 mm diameter), a water-cooled condenser, and a small collection flask. The flask was occasionally connected to an HPLC pump for fed-batch operation. The heating bath was set at 170 °C, and the actual reaction temperature was monitored in the reaction medium.

In a typical batch experiment, 1 g of zeolite powder (non-dried) was suspended in 50 g of 1-phenyl-ethanol (analytical grade, 98%) at room temperature and heated to the reaction temperature (170 °C) within a few minutes. As the reaction proceeded, several distillate fractions were collected, and samples were withdrawn from the residual suspension in the flask. The distillate consisted of two phases, an aqueous phase and a styrene-rich organic phase. The organic phase was analysed by gas chromatography (GC). The bottom samples contained some catalyst particles, which were allowed to settle before analysis. It should be mentioned that the most active catalysts started reacting at ∼155 °C and performed most of the conversion before the set temperature of 170 °C was reached. The high endothermicity of the reaction and product evaporation hampered rapid heating of the reaction mixture.

The catalyst library comprised various commercial and synthesized acidic materials, including amorphous silica–alumina, medium-pore zeolites (H-ZSM-5, H-ZSM-11, H-TON, H-PSH-3, H-FER, and the Lewis-acidic TS-1), and large-pore zeolites (H-Beta, H-Y, H-MOR, and SAPO-5). The Si/Al atomic ratio of the zeolites is given here as the number in parentheses after the zeolite name. For instance, H-ZSM-5(15) refers to an acidic ZSM-5 zeolite with a Si/Al ratio of 15. The Si/Al ratio was either provided by the manufacturer or determined using X-ray fluorescence.

The commercial zeolites were obtained from Zeolyst under the codes CBV-3020 for H-ZSM5(15), CBV-5020 for H-ZSM5(22), CBV-5534 for H-ZSM5(27), CBV-80 for H-Y(42), CP-504-20 for H-MOR(10), and CP-811B-200 for H-Beta(100). The silica–alumina was Criterion X-800.

The GC analyses were carried out using an apolar 50-m CP-Sil column that was run from 80 to 280 °C. The organic samples were diluted in toluene to which a small amount of *n*-decane was added as a standard. The yields were expressed as the molar fraction of the phenyl-ethanol intake that was converted to the product considered. Yields and conversion were integrated over the whole run length. The catalyst activity was expressed as space–time yield (STY) in $g_{styrene}/(g_{cat}\,h)$.

The mass and carbon balances typically closed between 85 and 95%. Occasionally, the carbon balance deviated significantly from the mass balance with respective closures to ∼40 C% and ∼90 wt%, for instance. Such large deviations indicate the formation of heavy components that did not elute during the GC analysis but are present in the liquid product.

3. Results

3.1. Catalyst screening

In a reference batch experiment, H-ZSM-5(15) was used at 2 wt% loading in 1-phenyl-ethanol at 170 °C. Analysis of the distillates and bottom products revealed the selective formation of styrene and water up to a conversion of ∼90 mol% and the formation of diphenyl-ethyl ethers and other heavy products (HE) beyond this point (Fig. 2). Ethylbenzene (EB) and acetophenone (AP) were formed in insignificant amounts. No cracking products, such as benzene, were observed. Styrene was distributed over the bottom and distillate fractions in a ratio of about 2:1. The reaction proceeded with an initial STY of ∼300 $g_{styrene}/(g_{cat}\,h)$, reached a maximum styrene yield of ∼85 mol%, and was completed within ∼15 min.

Most other catalysts operated with a lower reaction rate and/or followed less attractive yield–conversion profiles. Table 1 summarises the performance of selected catalysts in terms of initial activity (i.e., initial STY), maximum styrene yields (i.e., the maximum cumulative yield observed on increasing the conversion, as illustrated in Figs. 2b and 2c), and the carbon balance and mass balance achieved at the end of the experiment. In general, the medium-pore zeolites delivered higher maximum yields than the large-pore zeolites or mesoporous acids, such as amorphous silica-alumina and heteropolyacids. For example, the medium-pore zeolite H-ZSM-11, as well as the titano- and iron-silicates TS-1 and H-(Fe)ZSM-5, showed high maximum styrene yields. Although exhibiting similar activity, large-pore zeolites such as H-Beta and H-MOR showed poor selectivity for styrene. They preferably formed ethers and heavy products. For instance, H-MOR(10) produced mainly the ethers of phenyl-ethanol over a wide range of conversions. The ethers were then converted to heavy oligomeric products at higher

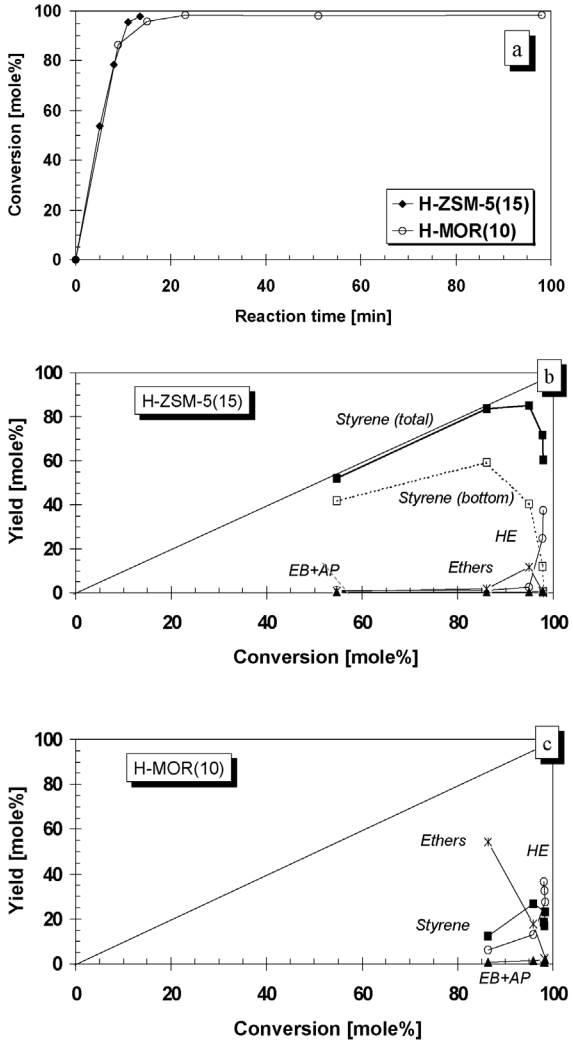

Fig. 2. Dehydration of phenyl-ethanol over H-ZSM5(15) and H-MOR(10) (batch reactive distillation, 170 °C; 2 wt% catalyst).

conversion (Fig. 2). A part of the heavy products did not elute from our GC columns, as indicated by poor carbon balances (40–50 C%; see Table 1) despite good mass balances.

3.2. Si/Al ratio

The Si/Al ratio appeared to be an important parameter for the H-ZSM-5 zeolite (Table 1; Fig. 3). The reaction rate and the styrene yield decreased with increasing Si/Al ratio. More specifically, the initial STY and maximum styrene yield dropped from ∼300 to ∼30 $g_{styrene}/(g_{cat}\,h)$ and from ∼85 to 25 mol%, respectively, when the Si/Al ratio increased from 15 to 150.

That this was not the only important parameter is demonstrated by the fact that a second batch, H-ZSM-5(15bis), showed lower activity and selectivity than the original H-ZSM-5 (15) batch (Fig. 3). Its initial rate and maximum yield amounted to ∼130 $g_{styrene}/(g_{cat}\,h)$ and 75 mol%, respectively, compared with ∼300 $g_{styrene}/(g_{cat}\,h)$ and 85 mol% for the original batch under identical conditions. The possible origin of this discrepancy is discussed later in this paper.

Table 1
Selected solid acid catalysts used in the dehydration of 1-phenyl-ethanol (batch reactive distillation, 170 °C, 2 wt% catalyst)

Name	Si/Al (mol/mol)	Max. yield (mol%)	Init. STY (g/(g h))	Balances	
				(C%)	(wt%)
Medium-pore zeolites					
H-ZSM-5	15	*85*	318	77	86
H-ZSM-5	22	*55*	48	73	87
H-ZSM-5	27	43	69	50	89
H-ZSM-5	150	25	30	58	89
H-(Fe)ZSM-5	–	*91*	197	99	85
TS-1	–	*70*	20	93	88
H-ZSM-11	60	44	100	76	92
H-TON	20	12	3	84	92
H-FER	10	34	27	45	92
H-PSH-3	15	12	38	40	92
Large-pore zeolites					
H-Y	42	12	7	35	95
H-MOR	10	27	46	54	92
H-Beta	100	19	21	63	96
Heulandite	–	10	14	45	92
SAPO-5	–	23	12	40	93
Non-zeolitic acids					
Silica–alumina	–	20	6	59	93
γ-Alumina	–	0	0	–	–
$H_3PW_{12}O_{40}$	–	25	44	63	90
$Cs_{2.5}H_{0.5}PMo_{12}O_{40}$	–	0.6	0.2	95	91
H–CuMg-sapionite	–	18	3	44	90

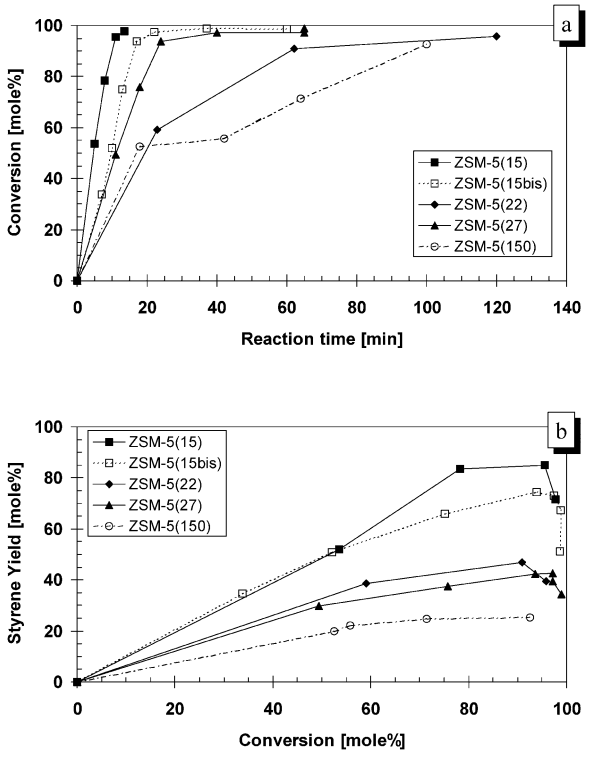

Fig. 3. Dehydration of phenyl-ethanol over H-ZSM-5 zeolites with varying Si/Al ratio (batch reactive distillation, 170 °C, 2 wt% catalyst).

3.3. Zeolite modifications

Zeolites are known to catalyze reactions through the Brönsted acid sites located inside the micropores and on the external

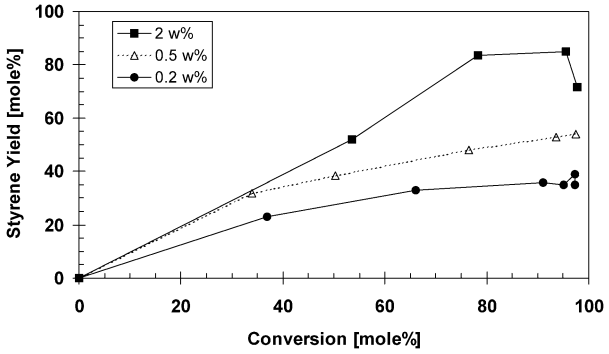

Fig. 4. Influence of catalyst loading on the styrene yield in the dehydration of phenyl-ethanol over H-ZSM-5(15) (batch reactive distillation, 170 °C; 0.2–0.5–2 wt% catalyst).

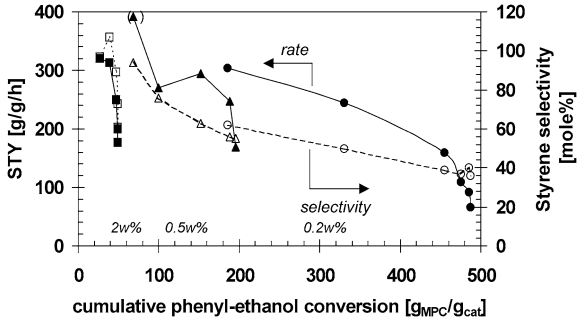

Fig. 5. Influence of catalyst aging over the styrene production rate and selectivity of H-ZSM-5(15) in the dehydration of phenyl-ethanol (batch reactive distillation, 170 °C, 0.2–0.5–2 wt% catalyst).

surface. The latter do not offer the confined environment or, consequently, the shape selectivity characteristic of the micropores. Hence, methods to passivate the external surface have been developed. One of these consists of a selective dealumination of the external surface by an aqueous solution of ammonium hexafluorosilicate (AHS), $(NH_4)_2SiF_6$ [10]. In the present study, this treatment was applied on zeolites H-ZSM-5(15) and H-ZSM5(55).

The AHS treatment did not affect the performance of the two ZSM-5 zeolites to any significant extent. For H-ZSM-5(15), the maximum yield and initial STY were 85 mol% and 312 g/(g h) before AHS treatment and 79 mol% and 372 g/(g h) after AHS treatment; for H-ZSM-5(55), these values were 43 mol% and 69 g/(g h) before AHS treatment and 52 mol% and 63 g/(g h) after AHS treatment.

3.4. Catalyst loading

To assess the stability of the H-ZSM-5(15), we ran experiments at lower catalyst loadings for longer reaction times. When the catalyst loading was reduced from 2 to 0.2 wt%, the reaction time to achieve deep conversion increased from 15 min to 2.5 h. As expected, the catalyst loading did not affect the initial reaction rate to a significant extent. For instance, the initial styrene production rate remained in the order of 300–400 $g_{styrene}/(g_{cat}\,h)$ in all three cases. The reaction did not proceed equally selectively, however; the maximum styrene yield decreased from 85 to 39 mol% (Fig. 4).

The catalyst loading not only affected the cumulative styrene yield, but also affected the effective concentration of styrene dissolved in the reaction medium. On decreasing the catalyst loading from 2 to 0.5 or 0.2 wt%, the concentration of styrene was decreased by distillatively removing styrene from the medium when generated at a rate of ∼5 g/min. This observation also indicates that the loss of selectivity cannot be attributed to the consecutive reaction of dissolved styrene, because the highest concentrations were achieved with the most selective operation, that is, the highest catalyst loading.

The yield–conversion profile observed for the different catalyst loadings can be easily explained by considering the catalyst aging in the various runs, however. We can indeed express the catalyst age in terms of workload (i.e., cumulative amount of feed converted), and find a monotonous decrease in styrene selectivity with increasing workload throughout the data gathered at various catalyst loadings (Fig. 5). The cumulative selectivity decreased to 50 mol% after a workload of ∼250 g/g. Obviously, a lower catalyst loading requires a higher workload to reach a given conversion level. This explains its lower selectivity reported in Fig. 4. Fig. 5 also shows that the cumulative STY is only moderately affected by the catalyst age, beyond the rate drops at the conversion levels of 50, 200, and 500 $g_{phenyl\text{-}ethanol}/g_{cat}$. These rate drops are related not to catalyst deactivation, but rather to the approach of full conversion in the respective experiments. The fact that the initial STY does not depend on catalyst loading further supports the insignificance of product boil-off and external mass transport as factors influencing the reaction rate.

Despite its lower activity, the TS-1 catalyst also showed promising styrene yields. Thus, we investigated stability as was done for the H-ZSM-5(15) catalyst. The selectivity of the TS-1 catalyst appeared to decrease more rapidly that of the H-ZSM-5(15); it dropped to 50 mol% after a workload of about 100 g of converted feed per 1 g of catalyst.

3.5. Fed-batch operation

The decreasing styrene selectivity with time and catalyst age was not an intrinsic feature of the batch-distillation mode of operation. We carried out the dehydration reaction under fed-batch distillation conditions using 2 wt% of H-ZSM-5(15) and continuously supplying fresh phenyl-ethanol to the reaction flask to keep the liquid level nearly constant. The observed decrease in selectivity with increasing time and catalyst age or workload nicely followed the profile reported in Fig. 5 for the batch-distillation operation.

4. Discussion

4.1. Shape selectivity

The medium-pore zeolites delivered a higher styrene yield than the large-pore zeolites or the mesoporous materials. Therefore, the dehydration of phenyl-ethanol seems to benefit from shape selectivity. This dehydration proceeds best in micropores that are large enough to accommodate phenyl-ethanol but small

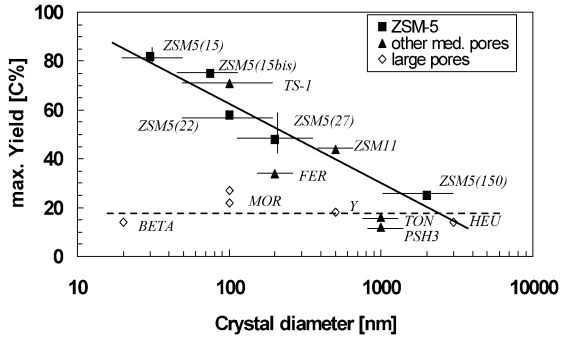

Fig. 6. Maximum styrene yield rate as function of the Al/Si ratio and crystal size d_p of medium-pore zeolites in the dehydration of phenyl-ethanol (batch reactive distillation, 170 °C, 2 wt% catalyst).

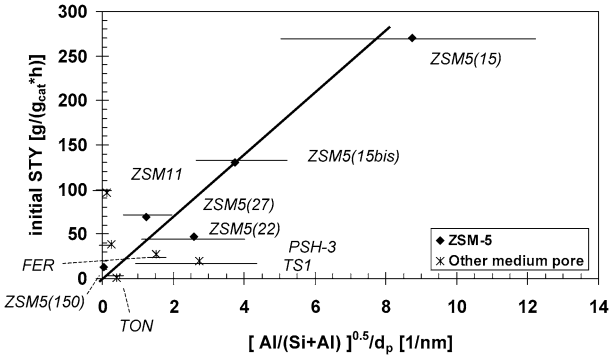

Fig. 7. Initial styrene production rate as function of the Al/(Si + Al) ratio and crystal size d_p of medium-pore zeolites in the dehydration of phenyl-ethanol (batch reactive distillation, 170 °C, 2 wt% catalyst).

enough to inhibit the formation of the bulky ethers and styrene oligomers (transition-state shape selectivity) or favouring their subsequent conversion to styrene through a slow diffusion out of the zeolite (product shape selectivity). With pore diameters of around 5.5 Å, medium-pore zeolites are indeed known to accommodate monoaromatics and exclude larger molecules such as polyaromatics [11].

The prominent role of the internal surface area is also confirmed by the activity and selectivity of AHS-treated zeolites. This treatment was supposed to passivate the external surface of the zeolite crystals by extracting the external Al atoms [10]; however, it did not affect the activity and selectivity of the zeolite to any significant extend. This also indicates that the external surface area of the zeolites is not responsible for the formation of the bulky ethers and oligomeric products.

Although we believe that shape selectivity plays an important role in determining the initial selectivity of the catalyst, it cannot explain all of the observations. We address this point later in the paper.

4.2. Si/Al ratio, crystal size, and pore structure

The catalytic performance of various H-ZSM-5 zeolites appeared to depend on the Si/Al ratio; the higher the Si/Al ratio, the lower the styrene yield (Fig. 3). This does not explain the difference between the H-ZSM-5(15) and H-ZSM-5(15bis) batches, however. The Si/Al ratio often correlates with changes in crystal size. During zeolite synthesis, Al-rich gels are indeed known to nucleate more rapidly than Al-lean gels, resulting in the formation of small crystals in the former case. The crystal size of the H-ZSM-5 used here indeed increased with increasing Si/Al ratio, from 20–50 nm for Si/Al = 15 to 1000–3000 nm for Si/Al = 150. Interestingly, the H-ZSM-5(15) and H-ZSM-5(15bis) differed slightly in crystal size (20–50 nm for the former vs. 50–100 nm for the latter). In fact, crystal size seems to have a greater influence on the catalytic properties of the ZSM-5 zeolites than the Si/Al ratio does. Both the maximum styrene yield and the styrene STY were found to decrease monotonically with increasing crystal size of the ZSM-5 zeolites, as illustrated in Fig. 6 for the maximum styrene yield. A very similar figure can be drawn for the initial STY. Fig. 6 describes particularly well the performance of the ZSM-5 series, with their varying Si/Al ratios, as well as the ZSM-11 and TS-1 materials. The FER, PSH-3, and TON zeolites delivered slightly lower yields at comparable crystal sizes. In contrast, the large-pore zeolites (open symbols) demonstrated no relationship between crystal size and maximum styrene yield. We discuss the physical basis for this observation in two steps, looking first at the initial rate and then at the maximum yield.

4.3. Zeolite activity

The relationship between crystal size and initial rate suggests that the reaction is rate-limited by intracrystalline diffusion and thus occurs close to the outer rim of the zeolite crystal. Mathematical models have been developed to describe the influence of diffusion on overall catalyst activity [12]. These models can be easily adapted to the present case. For the sake of argument, we assume that all ZSM-5 zeolites contain acid sites of identical nature and strength. (We discuss the validity of this argument later.) Accordingly, the intrinsic reactivity of the zeolite is expected to increase linearly with the Al/(Si + Al) ratio. When applied to catalysts with identical pore structures, diffusion models predict that the effective reactivity of a catalyst particle increases with the square root of its intrinsic activity and the inverse of the particle size [12]. Hence, we could reasonably expect the productivity of the ZSM-5 zeolites to follow Eq. (1):

$$\text{Initial STY} \sim A \cdot \left[\text{Al}/(\text{Si}+\text{Al})\right]^{0.5}/d_p. \quad (1)$$

Fig. 7 shows that indeed that Eq. (1) applies to the styrene productivity of the series of H-ZSM-5 zeolites (see the filled diamonds in Fig. 7). Equation (1) also explains semiquantitatively the difference in activity between H-ZSM-5(15) and (15bis). A more detailed inspection reveals, however, that the quality of the correlation depends mainly on $1/d_p$, which varies over nearly two orders of magnitude. In contrast, $[\text{Al}/(\text{Si}+\text{Al})]^{0.5}$ varies only over a factor ~3 and thus has a more limited impact. It should be noted that the data points were calculated for the centre of the crystal size distribution and thus are off-centre compared with the $1/d$ error bars.

Crystal size is not the only factor influencing the activity of the various medium-pore zeolites, because the other medium-pore zeolites did not fall on the "initial STY − [Al/(Si +

Al)$^{0.5}/d_p$" line found for the ZSM-5 zeolites (see the crosses in Fig. 7). The ZSM-11 zeolite was more active than a ZSM-5 of identical $[Al/(Si + Al)]^{0.5}/d_p$, whereas all other medium-pore zeolites showed lower activity.

The active H-ZSM-11 zeolite exhibits a pore structure very similar to that of the H-ZSM-5 (compare the MEL and MFI structures in earlier work [13]). It has a three-dimensional network of pores with a 5.3 × 5.4 Å aperture, compared with the three-dimensional network of 5.3 × 5.6 Å pores of the H-ZSM-5 zeolite. This could explain the comparable performance of these zeolites.

TS-1 shares the same pore and crystal structure as the ZSM-5 zeolites but is doped with Ti^{4+}- rather than Al^{3+}-atoms in the framework; thus Fig. 7 reports the $Ti/(Si + Ti)$ ratio instead of the $Al/(Si + Al)$ ratio for TS-1. Therefore, TS-1 is considered a solid Lewis acid rather than a Brönsted acid. The dehydration of alcohol does not seem to be a common property of Lewis acid catalysts; this reaction is not mentioned in reviews and textbooks on Lewis acids [14–16]. Lewis acids are reported to activate oxygenates in, for example, acetalisation and esterification reactions. They also tend to transform to Brönsted acids on reaction with the water produced by the dehydration reaction. This complicates assignment of the catalytic activity to either sort of acidity, because it requires that the acid sites be unambiguously characterised during the reaction. Therefore, the lower activity of TS-1 may be related to either the Lewis nature of its acidity or the weakness of its hydrated Brönsted form.

Ferrierite is characterized by a two-dimensional network of interconnected medium and small pores [13]. The medium pores are significantly narrower (4.2 × 5.4 Å) than those of ZSM-5. The poor activity of ferrierite suggests that its medium pores are too small to properly accommodate phenyl-ethanol or allow for its easy diffusion.

The TON zeolite has one-dimensional pores with ellipsoidal apertures (4.6 × 5.7 Å) [13]. Its low activity is due to its large crystal size and also possibly the one-dimensionality of its pores. These are readily blocked by the simple adsorption of one molecule at both apertures.

Finally, the PSH-3 zeolite (later renamed SSZ-25 or MCM-22) differs from the medium-pore zeolites discussed so far by having large elongated cages that are accessed through narrow medium-sized pores (4.0 × 5.5 and 4.1 × 5.1 Å) [13] resembling those of ferrierite. This similar pore structure could explain the similar activity of the two zeolites. However, the large cages probably offer enough room for the formation of ethers and styrene dimers, which are too large to escape the cage through the medium pores. The plugging of the cages might also contribute to the low activity of the PSH-3 zeolite.

We now need to consider the relevance of acid strength, which we explicitly neglected in our treatment. Earlier interpretations of variation in acid strength were based on the Sanderson electronegativity of the zeolite framework [17]; however, more recent work has revealed that zeolites show only a moderate variation in deprotonation energy [18]. In the case of gas-phase alkane conversion, the variation in acid strength seems to be dominated by the varying ability to "solvate" the cationic transition states in the zeolite micropores. The modified Thiele modulus defined above approximates the intrinsic zeolite activity by its $Al/(Si + Al)$ ratio, with no consideration of the strength of the corresponding acid sites or the solvation capabilities of the zeolite framework. Taking proper account of these factors might explain the difference in rate observed between the ZSM-5 zeolite series and the other medium-pore zeolites. Nevertheless, these refinements cannot overshadow the dominant influence of crystal size shown in Fig. 7, but at best can only modulate it.

4.4. Styrene yield and deactivation

The physical basis for the relationship between the maximum styrene yield and crystal size (Fig. 6) is not easy to rationalize. It cannot be attributed to an increased contribution of the external surface area in forming ethers and oligomeric materials, for passivation of the external surface area did not improve zeolite selectivity. Hence, we need to invoke other factors to explain the influence of crystal size on selectivity.

In fact, the maximum styrene yield has so far been taken as an indicator of the intrinsic selectivity of the catalyst. It this were the case, then the yield–conversion profile would be independent of catalyst loading, which contrasts with the findings shown in Fig. 4. The experiments with various catalyst loadings illustrated in Fig. 5 reveal that indeed the maximum yield is more a function of the deactivation rate of the catalyst. As the H-ZSM-5 zeolite converts more feed, it also loses selectivity toward styrene. The catalyst does not seem to lose much of its activity, however (Fig. 5). Hence the loss in selectivity should be seen as an increase in byproduct formation (particularly diphenyl-ethyl-ethers), rather than a decrease in styrene production. We can propose no simple model to satisfactorily explain all of these observations, however.

4.5. Liquid-phase versus gas-phase dehydration

The present study reveals important differences in behaviour compared to the gas-phase operation reported earlier [8,9]. Running the reaction under gas-phase conditions at 250–290 °C, equally high styrene selectivity was observed for small-, medium-, and large-pore zeolites (e.g., for SAPO-34, H-ZSM-5 and H-Beta). It was then concluded that the gas-phase reaction proceeds at the external surface of the zeolite crystals. The selectivity of SiO_2-bound ZSM-5 extrudates was affected by the slow diffusion of the product through the mesopores between the zeolite particles and SiO_2 binder. Low zeolite loadings in the extrudates were indeed required to achieve high selectivity and stability.

Such differences in behaviour can be explained qualitatively. The strong influence of pore size and crystal size reported here strongly indicates that the reaction at 170 °C is occurring inside the zeolite micropores and is rate-limited by the diffusion of reactant and product within these pores. Operation at higher temperature (220–250 °C) is therefore likely to result in more severe diffusion limitation, up to the point where reaction in the

micropores is no longer significant and the reaction becomes limited to the external zeolite surface.

Besides the increase in temperature, the switch from liquid phase to gas phase also may contribute to better performance by removing the background activity of the liquid phase that was speculated on earlier. Consequently, the reaction could proceed at higher selectivity (∼90 mol%) over a much longer lifetime (>150 h).

5. Conclusion

The dehydration of 1-phenyl-ethanol to styrene was carried out at mild temperature (170 °C) under reactive distillation conditions. The reaction proceeds with high rates (300 g styrene per 1 g of catalyst per h) and leads to styrene with high initial selectivity using ZSM-5 with very small (<50 nm) crystals (i.e., low Si/Al ratio). ZSM-11 zeolite, which exhibits very similar pore structure, shows comparable activity and styrene selectivity at comparable crystal size. Ferrierite and PSH-3 (also called MCM-22) show lower activity and selectivity, seemingly related to their narrower medium-sized pores. In contrast, large-pore zeolites do not form styrene to a significant extent. Therefore, styrene formation seems to be determined by the shape selectivity of the medium-pore zeolites. TS-1, a Lewis-acidic Ti-silicate equivalent of ZSM-5 zeolite, shows moderate activity but good selectivity for this reaction.

The styrene selectivity of these materials decreases rapidly with time on stream, resulting in the formation of diphenyl-ethyl ethers and, subsequently, oligomeric products. Operations with low zeolite loading (<1 wt%) in the slurry using ZSM-5 zeolites with high Si/Al ratios also result in enhanced formation of ethers. No simple model can explain all of the factors affecting ether formation.

Acknowledgments

The authors thank T.L.M. Maesen, presently working for Chevron, for valuable discussions and R.J. Haan for his invaluable technical assistance.

References

[1] A. Chauvel, G. Lefebvre, Petrochemical Processes: 1 Synthesis-Gas Derivatives and Major Hydrocarbons, Technip, Paris, 1989.
[2] W.L. Faith, D.B. Keyes, R.L. Clark, Industrial Chemicals, second ed., Wiley, New York, 1957.
[3] H.J. Sanders, H.F. Keag, H.S. McCullough, Ind. Eng. Chem. 45 (1953) 2.
[4] J.R. Skinner, C.E. Sanborn, DE 2146919 (1972), assigned to Shell. Int. Res.
[5] H. Dirkzwager, M. van Zwienen, WO 9958480 (1999), assigned to Shell Int. Res.
[6] G. Csomontanyi, A. Panovici, Rev. Roum. Chim. 17 (1972) 525.
[7] T. Takahashi, T. Kai, M. Tashiro, Can. J. Chem. Eng. 66 (1988) 433.
[8] J.-P. Lange, C.M.A.M. Mesters, Appl. Catal. A: Gen. 210 (2001) 247.
[9] G.C. van Giezen, J.-P. Lange, C.M.A.M. Mesters, WO 9942425 (1999), assigned to Shell Int. Res.
[10] A.P. Carvalho, M. Brotas de Carvalho, F. Ramôa Ribeiro, C. Fernandez, J.B. Nagy, E.G. Derouane, M. Guisnet, Zeolites 13 (1993) 462.
[11] C.N. Satterfield, Heterogeneous Catalysis in Industrial Practice, second ed., McGraw–Hill, New York, 1991.
[12] K. Kapteijn, G.B. Marin, J.A. Moulijn, Stud. Surf. Sci. Catal. 123 (1999) 375.
[13] W.H. Meier, D.H. Olson, Ch. Baerlocher, Zeolites 17 (1996) 1; see also www.iza-online.org.
[14] M. Santelli, J.M. Pons, Lewis Acids and Selectivity in Organic Synthesis, CRC Press, New York, 1996.
[15] H. Yamamoto, Lewis Acids in Organic Synthesis, Wiley–VCH, Weinheim, 2000.
[16] A. Corma, H. Garcia, Chem. Rev. 103 (2003) 4307.
[17] P.A. Jacobs, Catal. Rev.-Sci. Eng. 24 (1982) 415.
[18] F. Hasse, J. Sauer, Microporous Mesoporous Mater. 35 (6) (2000) 379.